RESEARCH ARTICLE | JUNE 07 2024

Creating and detecting observable QED plasmas through beam-driven cascade

Special Collection: Papers from the 65th Annual Meeting of the APS Division of Plasma Physics

Kenan Qu ; Nathaniel J. Fisch

Phys. Plasmas 31, 062102 (2024)
https://doi.org/10.1063/5.0205425

Creating and detecting observable QED plasmas through beam-driven cascade

Cite as: Phys. Plasmas **31**, 062102 (2024); doi: 10.1063/5.0205425
Submitted: 26 February 2024 · Accepted: 23 May 2024 ·
Published Online: 7 June 2024

Kenan Qu[a] and Nathaniel J. Fisch

AFFILIATIONS

Department of Astrophysical Sciences, Princeton University, Princeton, New Jersey 08544, USA

Note: This paper is part of the Special Collection: Papers from the 65th Annual Meeting of the APS Division of Plasma Physics.
Note: Paper JI1 1, Bull. Am. Phys. Soc. **68** (2023).
[a]Invited speaker. **Author to whom correspondence should be addressed:** kq@princeton.edu

ABSTRACT

Quantum electrodynamic (QED) plasmas, describing the intricate interplay of strong-field QED and collective pair plasma effects, play pivotal roles in astrophysical settings like those near black holes or magnetars. However, the creation of observable QED plasmas in laboratory conditions was thought to require ultra-intense lasers beyond the capabilities of existing technologies, hindering experimental verification of QED plasma theories. This paper provides a comprehensive review of recent studies outlining a viable approach to create and detect observable QED plasmas by combining existing electron beam facilities with state-of-the-art lasers. The collision between a high-density 30 GeV electron beam and a 3 PW laser initiates a QED cascade, resulting in a pair plasma with increasing density and decreasing energy. These conditions contribute to a higher plasma frequency, enabling the observation of $\sim$0.2% laser frequency upshift. This solution of the joint production-observation problem should facilitate the near-term construction of ultra-intense laser facilities both to access and to observe the realm of strong-field QED plasmas.

I. INTRODUCTION

The past decades have witnessed a surge in astrophysical observations, particularly in the context of electron–positron pair plasmas.[1–3] Notably, these plasmas, dynamically rich and formed in proximity to magnetars,[4–10] have been linked to the generation of fast radio bursts,[11–14] unraveling one of the most significant mysteries in astronomy.[15,16] Pair plasmas also play pivotal roles in multi-messenger astronomy[17–21] and neutron-star merging events.[22,23] In these astrophysical environments, the intricate interplay between strong-field quantum[24–26] and collective pair plasma effects results[27–29] in the formation of what is referred to as "QED plasma."[30–34] Here, QED plasma is defined as a state of matter that features electron–positron pairs that exhibit collective effects in strong-field QED environments. The dynamics of the QED pair plasma exhibit unique features compared to traditional electron–ion plasmas, primarily due to additional physical aspects such as radiation reaction, relativistic effects, symmetric charge properties, and high mobility under laser pressure. While the theoretical framework for QED plasma has been extensively developed, experimental validation poses significant challenges,[30,33] particularly in generating sufficiently dense electron–positron pairs. Nevertheless, the potential insights into the fundamental physics of these exotic plasmas make such endeavors crucial.

According to the QED theory, quantum vacuum becomes unstable with respect to decay into electron–positron pairs in the presence of a strong field above the Schwinger limit[35] $E_{cr} \cong 1.3 \times 10^{18}\mathrm{Vm}^{-1}$. This requirement significantly exceeds the current capabilities of laser technologies. To bridge this substantial field strength gap and approach the Schwinger limit, several approaches have been proposed, with a focus on leveraging relativistic boosting.[36,37] Among the most promising strategies for achieving controlled high pair number multiplications, two stand out: colliding two ultra-intense lasers[37–48] (notably in the presence of electron seeds), or colliding one laser with a high-energy electron beam.[49–57] By employing the nonlinear Breit–Wheeler process, dense electron–positron pairs could be generated within the laser spot size.

The threshold at which isolated pairs transition into a plasma depends on how collective effects are observed.[58] Pair plasmas, in this context, display features such as relativistic properties, local non-neutrality, and highly anisotropic momentum distributions. These distinctive characteristics arise from the interplay of the strong-field

environment and the symmetric properties of electrons and positrons. Additionally, the generated pair plasmas, at least in initial experimental explorations,[59,60] would have low density and small scales. As a result, conventional parameters used to describe electron–ion plasmas, such as Debye length and skin depth, may either be unobservable or inappropriate for capturing the unique properties exhibited by the QED plasma.

This invited paper reviews our recent studies[31,32,61–64] focused on creating QED pair plasma using existing technologies and optimizing conditions for observing the collective signature. Specifically, our attention is directed toward the QED cascade in a configuration involving a counterpropagating laser pulse and a high-energy electron beam. This configuration serves the dual purpose of creating QED plasma and detecting the plasma frequency through intricate details of changes in the laser spectrum. During both the pair creation and deceleration processes, the plasma frequency increases, leading to an upshift in the laser frequency and inducing a chirp in the laser spectrum. The signal of collective pair plasma effects is optimized when the laser reaches the threshold intensity of 10^{22}–$10^{23}\,\mathrm{W\,cm^{-2}}$ for the "pair-stopping" regime.[31,32] In this regime, the created pairs lose almost all of their longitudinal momentum, exhibiting the maximum plasma frequency. Remarkably, the pairs formed tend to organize into filaments near the laser axis due to the laser ponderomotive force. The filamentation[63] enables the maintenance of a high pair density over extended distances during laser–plasma interaction.

The development of ultra-intense laser facilities[65–67] for accessing strong-field QED has become an increasingly active topic in the past decade. This review highlights that using state-of-the-art lasers and current electron beams can not only generate a QED cascade but also produce a pair plasma exhibiting collective effects. Numerical simulations demonstrate that the collision of a petawatt class laser and a dense 30 GeV electron beam creates a collective plasma, inducing a $\sim$1% upshift in the driving laser frequency. Importantly, the plasma frequency is found to be solely dependent on the electron beam energy density, provided the laser intensity reaches the pair-stopping threshold. Therefore, the research suggests that efforts and resources should be prioritized in improving electron beam energy density to achieve a higher plasma frequency. This discovery strongly advocates for the co-location of high-energy electron beam accelerators and high-power laser facilities.[56,57]

This paper is organized as follows: In Sec. II, various approaches to creating QED plasmas are presented, and a comparison of the required parameters for generating observable collective signatures is provided. The focus is on beam–laser collisions, with an emphasis on reaching the pair-stopping regime and outlining the conditions for achieving it. An estimation of the created pair plasma frequency as a function of the electron beam energy density is presented, which was first reported in Ref. 31. Additionally, the potential use of structured light, analyzed in Ref. 62, to enhance the signature through an extended interaction time is explored. In Sec. III, an analysis is conducted on how the created pair plasmas and the laser mutually influence each other, leading to laser frequency upshift, intensity decrease, and pair density filamentation. Various techniques for experimentally detecting changes in the laser spectrum are discussed. The reviewed contents were reported in Refs. 32, 61, 63, and 64. In Sec. IV, we review a 3D particle-in-cell (PIC) simulation, first reported in Ref. 32 to demonstrate how a 3 PW laser and a 30 GeV dense electron beam can create a pair plasma, inducing observable changes in the laser spectrum. In Sec. V, we summarize the main conclusions and discuss potential experimental implementations. By addressing the questions of minimal creation conditions of QED plasma and effective detection methods, we offer a roadmap for future experiments exploring strong-field QED environments.

II. EXPERIMENTAL CONDITIONS FOR CREATING OBSERVABLE QED PLASMAS

Several experiments[44,68–70] have reported the creation of electron–positron pairs through the interaction of relativistic lasers with high-Z materials. In these collisions, "Bethe–Heitler" pair production[71,72] occurs at relatively low laser intensities of $10^{19}\mathrm{W\,cm^{-2}}$, owing to the low energy requirement. However, it should be noted that this process alone cannot generate a cascade, and the resulting pair plasma is contaminated by solid electrons. A recent experiment[73] has reported creating pair plasma using an ultrahigh-energy proton beam to collide with both low-Z and high-Z materials. Pairs are created through hadronic and electromagnetic cascades and also the "Bethe–Heitler" process. The created pair plasma has a dimension larger than the skin depth. Such pair plasma is known as a fireball plasma and would develop transverse current filamentation instability.[74–76] Nevertheless, detecting the micrometer scale density inhomogeneity and magnetic field is a nontrivial challenge.

There have also been suggestions of using the collision of two electron beams with extreme energy[36,77,78] (or using a dense solid plasma as an "image" beam[79]) to create electron positron pairs. The produced pairs could become very dense in the non-perturbative regime.[36] However, because of the high Lorentz factor of the high-energy pairs, observing collective plasma effects remains very challenging.

A. Laser–laser collision

A QED cascade in a controlled manner can be produced through the "Breit–Wheeler" process[80] using two approaches. The first approach involves two ultra-intense counterpropagating laser pulses overlapping in a region with stationary electrons.[42,47] The laser beat wave accelerates the electrons to relativistic velocities, enabling Lorentz boosting of the laser field to the Schwinger limit. When the electron Lorentz factor γ is sufficiently large such that the quantum nonlinear parameter $\chi \equiv \gamma E/E_{\mathrm{cr}} > 1$, the electrons emit high-energy photons that can decay into pairs.[81] The laser continues to accelerate the pairs, emitting more photons and creating more pairs in a cascaded manner until the laser field terminates or when the pairs escape.

The laser–laser collision for the QED cascade likely requires laser intensities of $10^{24}\mathrm{W\,cm^{-2}}$, corresponding to a peak laser amplitude $a_0 \equiv eE/(m_e c^2 \omega_0) \sim 10^3$, where ω_0 is the laser frequency. The created pairs would be quickly accelerated to high energy with Lorentz factors $\gamma \sim a_0$ if the colliding lasers are linearly polarized. Although radiation damping would reduce the scaling to $\gamma \gtrsim a_0^{3/4}$ if the colliding lasers are circularly polarized,[25,39] the Lorentz factor of near 10^3 nevertheless substantially suppresses the plasma frequency. If the pair number multiplication factor is smaller than 10^3, the pair plasma frequency could be even smaller than that of the stationary seed electrons. These challenges limit the means of detecting collective plasma effects.

B. Laser collision with an e^- beam

An alternative method for the "Breit–Wheeler" pair creation involves the collision of a high-energy electron beam and an intense laser, as illustrated in Fig. 1. This approach capitalizes on the high-energy output of electron accelerators capable of generating Lorentz factors $\gamma \gtrsim 10^5$. Thus, the Schwinger field becomes accessible to laser intensities of 10^{22}–$10^{23}\,\mathrm{W\,cm^{-2}}$ in the rest frame of the electrons. When the quantum nonlinear parameter $\chi = 2a_0\gamma(\hbar\omega_0)/(m_e c^2)$ exceeds unity, the electrons emit high-energy photons through a quantum radiation reaction. These emitted photons, if possessing sufficient energy, decay into an electron–positron pair in the strong field. Each pair particle can further emit more photons, creating a cascade of photon emission and pair creation. The cascade process converts pair energy into a larger particle number, terminating when the particle energy can no longer provide a sufficiently large Lorentz boost. Neglecting low-energy photons that cannot decay into pairs, the pair density n_p approximately follows the below scaling relation,

$$n_p \approx n_0\chi_0 = 4\times 10^{-6} a_0 n_0 \gamma_0, \tag{1}$$

for a micrometer wavelength laser, where n_0 and γ_0 are the density and energy of the injected electron beam, respectively, and χ_0 is the quantum nonlinear parameter of the initial electron beam in the peak laser field. χ_0 is also interpreted as the pair number multiplication factor. For a tens-of-giga-electron volt electron beam and 10^{22}–$10^{23}\,\mathrm{W cm^{-2}}$ laser, the pair multiplication factor can exceed 100.

The quantum radiation reaction, which induces a significant energy loss to the charged particles for each emission, has drastically different emission spectra compared to the classical radiation reaction. Moreover, the stochastic nature of the quantum radiation reaction causes a broadening of the particle momentum distribution,[64,82,83] in contrast to a narrowing distribution under the classical radiation reaction. Interestingly, the radiation reaction could enhance the acceleration of electrons and the absorption of laser through a strong plasma magnetic field.[84] Substantial efforts have been put into the experimental observation of the quantum radiation reaction and pair generation. The seminal E-144 experiment[59,60] at SLAC was already able to detect the quantum radiation reaction and pair generation using a $10^{18}\,\mathrm{W cm^{-2}}$ laser and a 50 GeV beam in the 1990s. Since then, the laser technology has rapidly grown, and the E-320 experiment[85] at the same facility is implementing $10^{20}\,\mathrm{W\,cm^{-2}}$ lasers. Future upgrades[56] of the facility contemplate a multi-petawatt laser colliding with an electron beam greater than 100 GeV. The LUXE experiment[86] at DESY is also proposing using a 17.5 GeV beam to collide with a 10^{20}–$10^{21}\,\mathrm{W\,cm^{-2}}$ laser pulse. Development of laser wake field accelerator (LWFA) technologies makes such collisions possible in high-intensity laser facilities. The Gemini laser facility[87,88] employed a $4\times 10^{20}\,\mathrm{W cm^{-2}}$ laser pulse colliding with a giga-electron volt electron beam, created via LWFA, to observe signatures of the quantum radiation reaction.

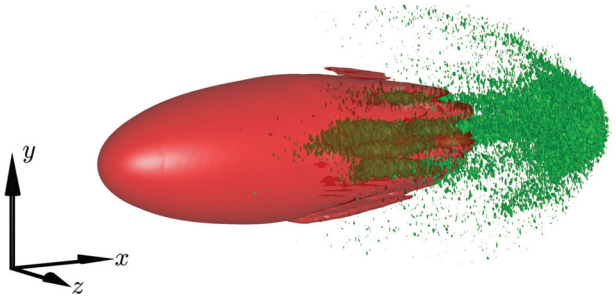

FIG. 1. A laser (red) propagating in the x direction collides with an electron beam to create a pair plasma (green). After collision, the pairs separate into two groups. One group quickly expands and continues to propagate in the beam direction. The other group is reflected and forms filaments near the center of the laser. [Reproduced with permission from Qu *et al.*, Phys. Rev. E **109**, 035208 (2024).]

C. Pair-stopping regime

The lower requirement for laser intensity in the beam-driven cascade is not only easier to build but also advantageous for producing stronger collective plasma effects. A higher plasma frequency $\omega_p \propto \sqrt{n_p/\gamma}$ is achieved by both increasing the pair density and reducing the pair energy. In a beam-driven cascade, the pair particles are continuously decelerated in the counterpropagating laser pulse through both photon emission and ponderomotive forces. Because the pair decay process becomes exponentially small when $\chi \lesssim 1$, but high-energy photon emissions remain relevant for pair dynamics until $\chi \sim 0.1$, the created pairs decelerate by emitting photons even after the QED cascade terminates. The optimal condition for the maximum plasma frequency is reached when the particle energy is fully converted into pair number multiplication and each particle loses almost all of its longitudinal momentum. This pair-stopping regime[31] is achieved when the laser exceeds the threshold intensity $I_{\mathrm{th}} \sim 10^{22}$–$10^{23}\,\mathrm{W cm^{-2}}$ and has a sufficiently long duration. When the quantum radiation reaction process terminates in such a strong laser field, the pair momentum is already sufficiently small that the laser ponderomotive force can change the pair direction. In this regime, the minimum pair energy is bounded by the quiver motion in the laser field, i.e., $\gamma_p \sim a_0$. Therefore, a lower laser intensity can reduce the minimum pair energy and lead to a higher pair plasma frequency.

Increasing the laser intensity above the threshold value I_{th} for pair stopping would simultaneously result in a proportionally larger pair number and higher pair energy, preventing the induction of a higher plasma frequency. Using Eq. (1) and $\gamma_p \sim a_0$, we find that the pair plasma frequency scales as

$$\omega_p \approx 2\times 10^{-3}\sqrt{n_0\gamma_0/n_c}, \tag{2}$$

where $n_c \sim 1.7\times 10^{21}\,\mathrm{cm^{-3}}$ represents the critical density for a 0.8μm laser. Hence, a high pair plasma frequency can only be achieved by employing electron beams with substantial energy density. Assuming a laser at the pair-stopping threshold intensity with $a_0 \sim 100$, the QED cascade can generate a pair plasma near the critical density if the electron beam has an energy density of $n_0\gamma_0 \sim 10^{25}\,\mathrm{cm^{-3}}$, corresponding to $10^{18}\,\mathrm{J\,cm^{-3}}$. The plasma frequency could reach $\omega_p \sim 0.02\omega$. For a tens-of-giga-electron volt-level electron beam, the density needs to exceed $10^{19}\,\mathrm{cm^{-3}}$. The high beam density requirement clearly favors conventional linear accelerators over the existing plasma accelerators.

D. Using Laguerre–Gaussian laser

As the electron beam and created pairs can be stopped by the laser fields if its intensity sustains above I_{th} for a sufficient duration, the QED cascade may terminate before the particles could traverse

through the entire laser pulse. Thus, for ultrahigh laser energies, a larger laser spot size could be more favorable than a higher peak intensity, yielding a larger pair multiplication number. A larger spot size also allows for the exploration of spatially structured laser pulses for a strong laser–plasma interaction. Mercuri-Baron *et al.*[89] investigated the use of Laguerre–Gaussian (LG) laser beams and found that their collision with an electron beam could yield a larger number of pair particles if the laser power is above a threshold value.

Using an LG laser beam could also mitigate pair plasma expansion and increase the laser–pair interaction time.[62] In contrast to a fundamental mode Gaussian beam, an LG beam has a donut-shaped intensity profile, creating a cylindrical ponderomotive potential for the pair particles. If the pairs are created on the inner side of the cylindrical potential, their transverse momentum would not overcome the potential and, hence, would be confined near the laser axis. The pair confinement not only mitigates pair scattering but also enhances the signature of collective plasma effects resulting from pair scattering inside the LG laser beam.

III. DETECTING SIGNATURES OF QED PLASMA EFFECTS

Detecting QED plasma effects in the laboratory poses challenges due to the extreme conditions of the QED cascade. The first challenge lies in the small plasma volume. Since lasers need to be tightly focused to provide the highest intensity, the cross section for pair creation is limited to a few square micrometers. Although the pair plasma volume would grow from expansion under the laser ponderomotive force, the expansion quickly dilutes the plasma, reducing plasma effects. Moreover, numerical simulations show that the pairs would form filaments[63] near the region of the peak laser intensity, further reducing the plasma cross section to sub-μm^2 levels.

The small plasma volume prevents the onset of plasma instabilities if the instability spatial scale exceeds the plasma wavelength. One example is the Weibel instability,[90–95] characterized by transverse density filamentation with a wavenumber near c/ω_p. Since $\omega_p \ll \omega_0$, the filamentation mode grows rapidly only if the transverse filament wavelength is much longer than the laser wavelength. For a pair plasma with a square micrometer cross section, the streaming currents cannot generate a sufficiently strong magnetic field to form density filaments, thus suppressing the instability.

The second challenge arises from the finite evolution time of the pair plasma. The pair particles are created with relativistic velocity and have a volume of a few micrometers per cube. Without an external confinement field, the pair volume grows exponentially at a picosecond timescale, and the rapid decrease in density inhibits the development of plasma instabilities with a lower growth rate. Near the center of a laser pulse, the ponderomotive force can focus the pairs into filaments and maintain their density. However, the laser–plasma interaction time is limited to the pulse duration, expected to be below ~ 100 fs, which corresponds to 40–50 laser periods. This duration is shorter than the timescales of processes, such as the two-stream instability $\tau_{\rm TS} \sim \gamma/\omega_p \sim 2300/\omega_0$ and the Weibel instability $\tau_{\rm W} \sim \sqrt{\gamma}/\omega_p \sim 100/\omega_0$.[93,94] The limited interaction time also prevents laser scattering through, for example, stimulated Brillouin scattering,[96] which requires over picosecond-long growth time.

The challenges are compounded by the kinetic pair dynamics under the influence of a strong laser field and radiation reaction. As the pairs are decelerated by the laser field, radiation reaction could lead to both heating and cooling of the pair plasma depending on the laser intensity.[64,82,83] Their momentum distribution becomes extremely anisotropic as the pairs are longitudinally stopped and partially reflected. The strong laser potential dominates the pair motion, preventing them from achieving thermal equilibrium during the interaction. Therefore, the collective effects cannot be described by parameters such as Debye length which is defined based on achieving an equilibrium state.

A. Laser frequency upshift

Given the substantial challenges, observing the collective effects of a QED pair plasma requires a method that is sensitive to an approximate micrometer per cube plasma volume, responds within several laser periods, and is robust to kinetic thermal effects. A noteworthy property of QED plasma is that the pair creation and deceleration processes occur inside the laser field. It is known that the sudden creation of plasma over space amounts to a temporal interface of refractive indices, through which the laser frequency is upshifted.[97–101] The frequency upshift is directly related to the increase in plasma frequency and can thus serve as a signature of the collective pair plasma effects.

The concept of laser frequency upshift in a dynamic medium was first studied in the 1950s,[102] but its association with plasma creation was introduced in the 1970s,[103–105] with experiments reported in the 1990s and thereafter.[106–113] Laser frequency upshift is analogous to the process of laser wavelength shift when transmitting through a spatial interface of different refractive indices. When a plasma is suddenly created in the laser field, the laser spatial parameters, including its wavelength, must not change while its temporal parameter, including frequency, changes according to the decreasing refractive index. In the case of growing pair plasma of a few laser wavelengths, the increased laser phase velocity in the created plasma compresses the laser wavefront toward the front and causes a chirp in the laser spectrum.

Pair plasma causes a laser frequency upshift by creating a transverse current responsible for electric polarization. Each pair particle created in the strong laser field is driven to a transverse oscillation at the laser frequency. The pair transverse momentum is determined by the laser field vector potential A, i.e., $p_\perp = eA_\perp$, assuming they have no initial transverse momentum at creation. The pair transverse current is, thus, $J_\perp = 2en_p p_\perp/(\gamma m_e) = \epsilon_0 \omega_p^2 A_\perp$, where ϵ_0 is the vacuum permittivity and $\omega_p = [2n_p e^2/(\gamma m_e \epsilon_0)]^{1/2}$ is the pair plasma frequency. The evolution of the laser field is governed by the wave equation with a time-dependent value $\omega_p(t)$,

$$\nabla^2 A_\perp - \frac{1}{c^2}\partial_t^2 A_\perp = \frac{\omega_p^2}{c^2} A_\perp. \tag{3}$$

As ω_p changes non-adiabatically in time, the laser frequency varies to obey the dispersion relation $\omega^2 = c^2k^2 + \omega_p^2$. Thus, the sudden creation of pair plasmas upshifts the laser frequency by an amount $\omega_p^2/(2\omega)$ for $\omega_p \ll \omega$.

The relationship between plasma creation and laser frequency upshift can be intuitively explained in a spacetime diagram,[61] as shown in Fig. 2. The parallel lines represent the laser wavefront propagating in the x direction, and their horizontal and vertical separation describes the laser wavenumber and frequency, respectively. The laser propagates through a growing plasma denoted by the shaded region. In the plasma, the laser phase velocity $v_p = c/(1 - \omega_p^2/\omega^2)^{1/2}$ changes, denoted by variations in the slopes. The increase in v_p in a

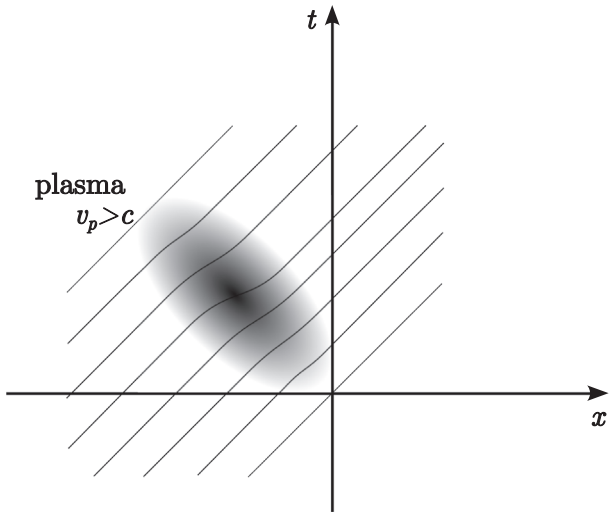

FIG. 2. Spacetime diagram of plasma creation and laser frequency upshift. [Reproduced with permission from Qu *et al.*, Plasma Phys. Control. Fusion **65**, 034007 (2023).]

growing plasma compresses the laser wavefront, indicating frequency upshift. However, the plasma density decreases in the tail, which stretches the laser wavefront, causing a frequency downshift. The laser spectrum is chirped after propagating through a small plasma.

The laser chirping profile can be analytically modeled by tracing the amount of phase shift induced by the varying plasma frequency.[61] Working in a comoving frame $\xi = x - ct$ and $\tau = t$, the laser phase is written as $\phi = -\omega\xi/v_p + \omega(1 - c/v_p)\tau$. As the propagation time τ increases, the varying plasma frequency causes a variation in the phase $d\phi = (1 - c/v_p)d\tau \approx (\omega_p^2/\omega)d\tau$. Because each part of the laser at ξ propagates through plasmas at $(\xi + c\tau', \tau')$, the total phase shift is $\Delta\phi = \int_{-\infty}^{\tau} \omega_p^2(\xi + \tau', \tau')d\tau'$. Transforming to the lab frame using $\partial_t = \partial_\tau - c\partial_\xi$ and $\partial_x = \partial_\xi$, we find

$$\Delta\omega(x,t) = \partial_t\Delta\phi = \frac{1}{2\omega}\int_{-\infty}^{t}\left[\partial_T\omega_p^2(X,T)\right]_{X=x-ct+ct'}^{T=t'}dt', \tag{4}$$

$$\Delta k(x,t) = \partial_x\Delta\phi = -\frac{1}{2\omega}\int_{-\infty}^{t}\left[\partial_X\omega_p^2(X,T)\right]_{X=x-ct+ct'}^{T=t'}dt'. \tag{5}$$

The shifts in frequency and wavenumber are the integral over the temporal and spatial change of ω_p^2 in the retarded position X, respectively.

B. Pair reflection and double Doppler shift

For a given pair number multiplication, the frequency upshift could be maximized by reducing the pair energy. The detectable signature of plasma effects is optimized in the pair-stopping regime by adopting a laser above the threshold intensity $I_{\rm th}$. In this regime, the pairs lose almost all of their longitudinal momentum and have the minimum Lorentz factor. However, the pairs could be reflected and reaccelerated by the laser if the pairs have a lower initial energy or if the laser pulse has a longer duration.

Interestingly, reacceleration of the pairs, despite the increased Lorentz factor, further upshifts the laser frequency. The increased laser frequency upshift in the pair-reflection regime could be explained through Doppler shift. The laser frequency upshift could be written as $\Delta\omega/\omega = \int_{-\infty}^{t}\partial_T[\omega_p^2(X,T)/\omega^2(X,T)]dt'$. Note that the plasma frequency $\omega_p \propto \sqrt{n_p/\gamma}$ is invariant under frame transform. However, the laser frequency ω decreases by a factor $1 + \beta$ when transforming to the rest frame of the reaccelerated pairs, where β is the pair velocity in the unit of c. Therefore, reacceleration of the pairs could increase the laser frequency upshift by up to a factor of two compared to fully stopped pairs.

C. Pair filamentation and laser scattering

In the beam-driven QED cascade, the pair plasma is initially created within a small sphere near the electron beam, typically having a diameter smaller than or similar to the laser wavelength. When the plasma frequency becomes non-negligible, it induces Mie scattering of the laser toward larger angles. The scattered light beats with the driving laser pulse, modulating the laser intensity. This modulation leads to a strong ponderomotive potential that expels the pairs toward low-intensity regions. Simultaneously, the laser is refracted toward regions with lower plasma density, coupling to the pair redistribution and inducing ponderomotive filamentation. The filamentation instability[114–117] of relativistic plasma streams, considered one of the fastest growing modes, continuously develops when copropagating with the laser in the "pair-reflection" regime. It eventually confines the reflected pairs into a few filaments, as shown in Fig. 1, each with a diameter near the laser wavelength.

The consequence of pair filamentation is strong laser scattering toward larger angles and continuous laser energy loss.[63] The pairs diffract laser energy via both Thompson scattering and Mie scattering. In the beginning stage of the QED cascade, the small pair plasma can be modeled as a δ function in space. The pair oscillation in synchrony radiates like a relativistic dipole and causes Thompson scattering. The radiation predominantly emits in the direction perpendicular to the laser polarization and is skewed toward the pair propagation direction. As the dimensions of the pair plasma grow, it transforms into Mie scattering, which is less polarization dependent but remains anisotropic.

Because the filaments are aligned with the laser axis, the continuous scattering causes a significant decrease in peak laser intensity. Near the pair-stopping point, the laser intensity I evolves as

$$\left\langle \frac{dI}{d\varphi} \right\rangle = -\frac{n_p}{\gamma n_c}\langle I\rangle, \tag{6}$$

where φ denotes the laser phase. If the pair plasma frequency reaches 0.1% of the laser frequency, i.e., $2\pi n_p/(\gamma n_c) \sim 0.2$, the peak laser intensity decreases by half within less than four laser cycles.

It is noted that a recent study[118] has shown that the nonlinear transverse motion of plasma filaments can yield accumulation of electron polarization through the asymmetry of radiative spin flips. The plasma filaments eliminate the need for an asymmetric field for producing spin-polarized plasmas,[119–121] uncovering the intrinsic existence of electron spin polarization during a γ-ray burst.

D. Signal detection

A notable implication of laser scattering is that it allows using an off-axis detector to collect the scattered wave and analyze the laser spectrum. The angle offset also prevents high-energy photons from directly hitting the spectrum analyzer causing damage. Since an optical spectrum analyzer can easily resolve a frequency shift of 10^{-4}, the constraint is rooted in the spectrum fluctuation of ultrahigh-power lasers. Nevertheless, even an observation of a 10^{-3} frequency upshift can reveal the creation of a near-critical density pair plasma, assuming that the pair Lorentz factor and the laser amplitude a_0 are in the range of 100.

In a QED cascade, the pair density and pair energy only rapidly change near the center of the laser pulse. According to Eq. (4), the laser frequency upshift is confined only to a fraction of the whole laser pulse duration. Thus, a much larger frequency upshift can be detected using a transient spectrum analyzer. Experimental detection typically uses techniques like frequency-resolved optical gating or spectral shear interferometry for a direct electric field reconstruction.

An even more sensitive measurement[32] of laser wavefront shift can be obtained using an interferometer, as sketched in Fig. 3. A small portion of the laser is split as a reference beam, which is combined with the driving laser after the collision. If the pair plasma induces a phase shift $\Delta\varphi$ in the driving laser field, the interference signal $I_{\rm int} \propto \Delta\varphi I_r$, where I_r is the intensity of the reference beam. The change in frequency $\Delta\omega$ can be found by differentiating the obtained phase change $\Delta\varphi$.

IV. NUMERICAL DEMONSTRATION

The upshift of laser frequency becomes experimentally observable by co-locating an electron beam with energy density $\gamma_0 n_0 \sim 10^{25}\text{cm}^{-3}$ and a laser pulse with intensity of $\sim 10^{22}\text{Wcm}^{-2}$. These conditions can be provided by "state-of-the-art" electron beam facilities and high-power laser facilities. For example, such an energy scale could be reached at SLAC by upgrading the FACET-II laser to 3 PW power with a waist of 3 μm. This laser is more than one order of magnitude lower than the intensities required for the all-optical approach. The electron beam can be provided by the LCLS-Cu RF LINAC[122] with 30 GeV energy and nanocoulomb charge. When focused into a sphere with 1 μm diameter, the electron beam can reach a peak density of $4 \times 10^{20}\text{cm}^{-3}$. According to scaling relation in Eq. (2), the beam-laser collision could create a pair plasma with $\omega_p \approx 0.075\omega$ to induce a laser frequency shift of $\Delta\omega/\omega \approx 0.56\%$.

The proposed electron beam-laser collision was numerically verified[32] using the QED PIC code EPOCH.[123] The parameters of the Gaussian laser pulse and electron beam are detailed in Table I. The laser is linearly polarized in the y direction and propagates along the x axis, while the electron beam moves in the opposite $-x$ direction. The simulation box measures $100 \times 30 \times 30\ \mu\text{m}^3$ and is discretized into $4000 \times 300 \times 300$ cells. The time step is 0.083 fs, with over 6×10^8 computational particles involved.

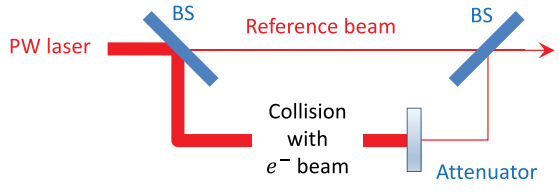

FIG. 3. Interferometer setup for the detection of the laser phase change. BS: beam splitter. [Reproduced with permission from Qu *et al.*, Phys. Plasmas **29**, 042117 (2022).]

TABLE I. The parameters of the laser and electron beam. The electron beam has a Gaussian distribution in all three space dimensions.

Laser	
Power	3 PW
Peak intensity	$3 \times 10^{22}\ \text{Wcm}^{-2}$
Duration	50 fs
Waist	2.5 μm
e^- beam	
Energy	30 GeV
Charge	1 nC
Beam size	$(1\ \mu\text{m})^3$
Peak density	$4 \times 10^{20}\ \text{cm}^{-3}$

The collision creates a pair plasma with a total charge of 26 nC and a peak density of $6.8 \times 10^{21}\ \text{cm}^{-3}$. The parameter determining the plasma frequency, n_p/γ, reaches a peak value of $2.4 \times 10^{19}\ \text{cm}^{-3}$, corresponding to 1.4% of the critical density of the driving laser. The density plot in Fig. 4(d) depicts the pair distribution in the $z = 0$ plane. Additionally, we highlight regions with $n_p/\gamma > 1 \times 10^{19}\text{cm}^{-3}$ using red dots in Figs. 4(a) and 4(b). The pair distribution showcases a hollow structure in the $z = 0$ plane, influenced by the strong ponderomotive force of the tightly focused laser. The inhomogeneous plasma

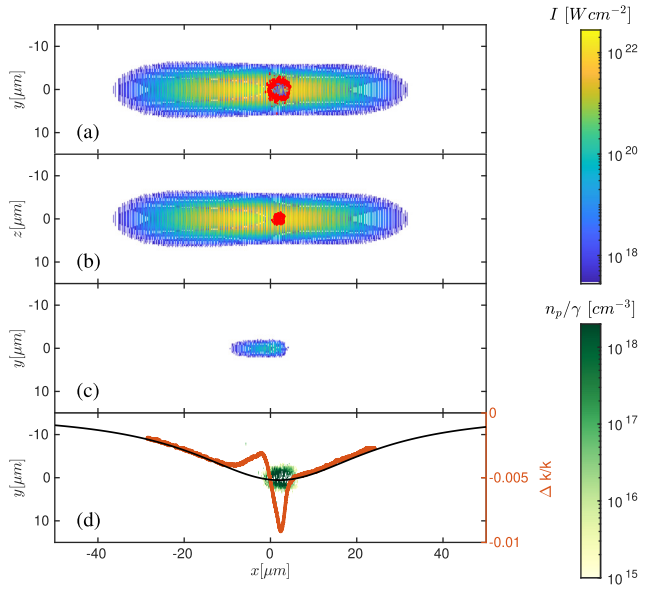

FIG. 4. The laser intensity profile at the $z = 0$ cross section (a) and $y = 0$ cross section (b). The red dots show the regions of $n_p/\gamma > 1 \times 10^{19}\text{cm}^{-3}$. The interference signal (c) and pair plasma parameter n_p/γ (d) at the $z = 0$ cross section. The red and black curves show the instantaneous wave vectors of the laser field at $y = z = 0$ with and without encountering the electron beam, respectively. [Reproduced with permission from Qu *et al.*, Phys. Plasmas **29**, 042117 (2022).]

distribution reveals a larger expansion in the plane of laser polarization. Pair filamentation is not developed in this simulation but it is formed in a separate 3D PIC simulation[31,63] with a large lase spot size 5 μm.

The creation of pair plasma is evident from both the altered laser spectrum and the interference signal. The simulation illustrates a maximum laser wavenumber upshift of 0.2%, represented by the red curve in Fig. 4(d). Since $\omega = ck$ outside the plasma, the wavenumber upshift is equivalent to a laser frequency upshift. In the case of an interferometer setup, as depicted in Fig. 3, the interference signal [Fig. 4(c)] reveals a peak signal intensity of $5 \times 10^{19}\,\mathrm{W cm^{-2}}$. Analyzing the slope of the signal intensity profile, a frequency upshift of approximately 0.16% is obtained.

To simulate the QED processes, the code EPOCH uses the locally constant field approximation (LCFA).[124,125] It is most accurate when the formation length of the QED processes are much shorter than the laser wavelength, which well suits the parameters of our interest. Note that, if the laser amplitude is moderately strong ($a_0 \sim 1$), the wavelength-scale interference effects would become important and simulation will be more accurate under the locally monochromatic approximation (LMA).[126,127]

V. SUMMARY

In summary, we have reviewed recent studies on the creation and observation of an electron–positron pair plasma through a beam-driven QED cascade. Comparing this approach to the all-optical method, the use of a high-energy density electron beam can significantly reduce the required laser intensity by over one order of magnitude, making it accessible to state-of-the-art laser technology. The counterpropagating geometry of the laser and pairs simultaneously increases pair density and decreases pair energy, contributing to a higher plasma frequency. The lower laser intensity also allows the created pairs to have lower Lorentz factors, making their collective effects observable at a lower density.

The signatures of collective plasma effects manifest in the intricate details of the laser spectrum as the pairs traverse through the laser pulse. The creation of plasma leads to a non-adiabatic reduction in refractive index, resulting in an upshift in the laser frequency that can be observed using a spectrum analyzer. In cases where the size of the pairs is smaller than the laser pulse, they induce a chirp in the laser spectrum characterized by an up-chirp followed immediately by a down-chirp, which can be detected using a transient spectrum analyzer. Additionally, a more sensitive measurement of the laser wavefront shift can be achieved using an interferometer.

In the configuration envisioned here, higher laser intensity does not more readily access the QED plasma regime through the pair multiplication factor in a QED cascade. Rather, the frequency of the created pair plasma depends solely on the electron beam's energy density, as long as the laser intensity exceeds the pair-stopping threshold of approximately 10^{22}–$10^{23}\,\mathrm{W cm^{-2}}$. Higher laser intensities simultaneously result in a larger pair density and higher pair energy, but these effects cancel each other out in their contribution to the plasma frequency. It is estimated that the collision of a 3 PW laser and an $10^{18}\,\mathrm{J\,cm^{-3}}$ electron beam can create a pair plasma and induce a 0.2% laser frequency upshift, a result demonstrated by 3D PIC simulations.

Our findings strongly advocate for the co-location of high-power lasers and high-energy output electron beam facilities. For instance, considering that the 2 nC, 30 GeV electron beam at SLAC could potentially be compressed into $0.5\,\mu\mathrm{m} \times (3\,\mu\mathrm{m})^2$, it could achieve an energy density of approximately $\sim 10^{18}\,\mathrm{J\,cm^{-3}}$. A collision between this electron beam and a 3 PW laser with a 2.5 μm waist could cascade into 26 nC pairs with a peak density of $6.8 \times 10^{21}\,\mathrm{cm^{-3}}$, resulting in a 0.2% shift in the laser frequency.

The laser wake field accelerator (LWFA) stands out as a promising technology capable of generating beam-driven QED cascades within an all-optical facility. Over the past decades, significant progress has been made in LWFA development, leading to the achievement of multi-giga-electron volt electron beam energies,[128–130] although the charge number is presently limited to the picocoulomb range. If LWFA can overcome the inherent trade-off between beam energy and charge number, a single petawatt laser facility could potentially generate detectable QED plasmas.

Beyond the scope of this review, we notice other studies on collective pair plasma dynamics emphasizing the effects of the quantum radiation reaction. For example, Liseykina *et al.*[131] investigates the inverse Faraday effect driven by radiation friction and its creation of multi-gigagauss magnetic fields. Bilbao and Silva[132] discover coherent radiation emission from kinetic plasma dynamics due to population inversion. Zhdankin *et al.*[133] report synchrotron firehose instability arising from the pressure anisotropy of synchrotron radiation.

ACKNOWLEDGMENTS

We acknowledge our collaborators S. Meuren and A. Griffith. This work was supported by NSF Grant No. PHY-2206691.

AUTHOR DECLARATIONS

Conflict of Interest

The authors have no conflicts to disclose.

Author Contributions

Kenan Qu: Funding acquisition (supporting); Writing – original draft (lead); Writing – review & editing (equal). **Nathaniel J. Fisch:** Funding acquisition (lead); Writing – original draft (supporting); Writing – review & editing (equal).

DATA AVAILABILITY

Data sharing is not applicable to this article as no new data were created or analyzed in this study.

REFERENCES

[1]A. Y. Chen, F. Cruz, and A. Spitkovsky, "Filling the magnetospheres of weak pulsars," Astrophys. J. **889**, 69 (2020).
[2]A. N. Timokhin and A. K. Harding, "On the maximum pair multiplicity of pulsar cascades," Astrophys. J. **871**, 12 (2019).
[3]R. Gueroult, Y. Shi, J.-M. Rax, and N. J. Fisch, "Determining the rotation direction in pulsars," Nat. Commun. **10**, 3232 (2019).
[4]V. M. Kaspi and A. M. Beloborodov, "Magnetars," Annu. Rev. Astron. Astrophys. **55**, 261 (2017).
[5]B. Cerutti and A. M. Beloborodov, "Electrodynamics of pulsar magnetospheres," Space Sci. Rev. **207**, 111 (2017).
[6]L. Lin, C. F. Zhang, P. Wang, H. Gao, X. Guan, J. L. Han, J. C. Jiang, P. Jiang, K. J. Lee, D. Li, Y. P. Men *et al.*, "No pulsed radio emission during a bursting phase of a Galactic magnetar," Nature **587**, 63 (2020).
[7]A. Ridnaia, D. Svinkin, D. Frederiks, A. Bykov, S. Popov, R. Aptekar, S. Golenetskii, A. Lysenko, A. Tsvetkova, M. Ulanov, and T. L. Cline, "A peculiar

hard x-ray counterpart of a galactic fast radio burst," Nat. Astron. **5**, 372 (2021).
[8]C. K. Li, L. Lin, S. L. Xiong, M. Y. Ge, X. B. Li, T. P. Li, F. J. Lu, S. N. Zhang, Y. L. Tuo, Y. Nang *et al.*, "HXMT identification of a non-thermal x-ray burst from SGR J1935 + 2154 and with FRB 200428," Nat. Astron. **5**, 378 (2021).
[9]C. D. Bochenek, V. Ravi, K. V. Belov, G. Hallinan, J. Kocz, S. R. Kulkarni, and D. L. McKenna, "A fast radio burst associated with a Galactic magnetar," Nature **587**, 59 (2020).
[10]The CHIME/FRB Collaboration, "A bright millisecond-duration radio burst from a Galactic magnetar," Nature **587**, 54 (2020).
[11]B. Marcote, K. Nimmo, J. W. T. Hessels, S. P. Tendulkar, C. G. Bassa, Z. Paragi, A. Keimpema, M. Bhardwaj, R. Karuppusamy, V. M. Kaspi *et al.*, "A repeating fast radio burst source localized to a nearby spiral galaxy," Nature **577**, 190 (2020).
[12]The CHIME/FRB Collaboration, "A second source of repeating fast radio bursts," Nature **566**, 235 (2019).
[13]V. Ravi, M. Catha, L. D'Addario, S. G. Djorgovski, G. Hallinan, R. Hobbs, J. Kocz, S. R. Kulkarni, J. Shi, H. K. Vedantham, S. Weinreb, and D. P. Woody, "A fast radio burst localized to a massive galaxy," Nature **572**, 352 (2019).
[14]K. W. Bannister, A. T. Deller, C. Phillips, J.-P. Macquart, J. X. Prochaska, N. Tejos, S. D. Ryder, E. M. Sadler, R. M. Shannon, S. Simha *et al.*, "A single fast radio burst localized to a massive galaxy at cosmological distance," Science **365**, 565 (2019).
[15]J. M. Cordes and S. Chatterjee, "Fast radio bursts: An extragalactic enigma," Annu. Rev. Astron. Astrophys. **57**, 417 (2019).
[16]E. Petroff, J. W. T. Hessels, and D. R. Lorimer, "Fast radio bursts," Astron. Astrophys. Rev. **27**, 4 (2019).
[17]M.-H. Wang, S.-K. Ai, Z.-X. Li, N. Xing, H. Gao, and B. Zhang, "Testing the hypothesis of a compact-binary-coalescence origin of fast radio bursts using a multimessenger approach," Astrophys. J. **891**, L39 (2020).
[18]B. P. Abbott, R. Abbott, T. D. Abbott, S. Abraham, F. Acernese, K. Ackley, C. Adams, R. X. Adhikari, V. B. Adya, C. Affeldt *et al.*, "GW190425: Observation of a compact binary coalescence with total mass $\sim 3.4 M_{\odot}$," Astrophys. J. **892**, L3 (2020).
[19]LIGO Scientific Collaboration and Virgo Collaboration. "GW170817: Observation of gravitational waves from a binary neutron star inspiral," Phys. Rev. Lett. **119**, 161101 (2017).
[20]C. Palenzuela, L. Lehner, M. Ponce, S. L. Liebling, M. Anderson, D. Neilsen, and P. Motl, "Electromagnetic and gravitational outputs from binary-neutron-star coalescence," Phys. Rev. Lett. **111**, 061105 (2013).
[21]M. Anderson, E. W. Hirschmann, L. Lehner, S. L. Liebling, P. M. Motl, D. Neilsen, C. Palenzuela, and J. E. Tohline, "Magnetized neutron-star mergers and gravitational-wave signals," Phys. Rev. Lett. **100**, 191101 (2008).
[22]Y. Q. Xue, X. C. Zheng, Y. Li, W. N. Brandt, B. Zhang, B. Luo, B. B. Zhang, F. E. Bauer, H. Sun, B. D. Lehmer, X. F. Wu, G. Yang, X. Kong, J. Y. Li, M. Y. Sun, J. X. Wang, and F. Vito, "A magnetar-powered X-ray transient as the aftermath of a binary neutron-star merger," Nature **568**, 198 (2019).
[23]D. J. Price and S. Rosswog, "Producing ultrastrong magnetic fields in neutron star mergers," Science **312**, 719 (2006).
[24]A. Di Piazza, C. Müller, K. Z. Hatsagortsyan, and C. H. Keitel, "Extremely high-intensity laser interactions with fundamental quantum systems," Rev. Mod. Phys. **84**, 1177–1228 (2012).
[25]A. Gonoskov, T. G. Blackburn, M. Marklund, and S. S. Bulanov, "Charged particle motion and radiation in strong electromagnetic fields," Rev. Mod. Phys. **94**, 045001 (2022).
[26]A. Fedotov, A. Ilderton, F. Karbstein, B. King, D. Seipt, H. Taya, and G. Torgrimsson, "Advances in QED with intense background fields," Phys. Rep. **1010**, 1–138 (2023).
[27]D. B. Melrose and R. Yuen, "Pulsar electrodynamics: An unsolved problem," J. Plasma Phys. **82**, 635820202 (2016).
[28]D. A. Uzdensky and S. Rightley, "Plasma physics of extreme astrophysical environments," Rep. Prog. Phys. **77**, 036902 (2014).
[29]D. Uzdensky, M. Begelman, A. Beloborodov, R. Blandford, S. Boldyrev, B. Cerutti, F. Fiuza, D. Giannios, T. Grismayer, M. Kunz, N. Loureiro, M. Lyutikov, M. Medvedev, M. Petropoulou, A. Philippov, E. Quataert, A. Schekochihin, K. Schoeffler, L. Silva, L. Sironi, A. Spitkovsky, G. Werner, V. Zhdankin, J. Zrake, and E. Zweibel, "Extreme plasma astrophysics," arXiv:1903.05328 (2019).
[30]P. Zhang, S. S. Bulanov, D. Seipt, A. V. Arefiev, and A. G. R. Thomas, "Relativistic plasma physics in supercritical fields," Phys. Plasmas **27**, 050601 (2020).
[31]K. Qu, S. Meuren, and N. J. Fisch, "Signature of collective plasma effects in beam-driven QED Cascades," Phys. Rev. Lett. **127**, 095001 (2021).
[32]K. Qu, S. Meuren, and N. J. Fisch, "Collective plasma effects of electron-positron pairs in beam-driven QED cascades," Phys. Plasmas **29**, 042117 (2022).
[33]H. Chen and F. Fiuza, "Perspectives on relativistic electron-positron pair plasma experiments of astrophysical relevance using high-power lasers," Phys. Plasmas **30**, 020601 (2023).
[34]M. V. Medvedev, "Plasma modes in QED super-strong magnetic fields of magnetars and laser plasmas," arXiv:2309.07316 (2023).
[35]J. Schwinger, "On gauge invariance and vacuum polarization," Phys. Rev. **82**, 664 (1951).
[36]V. Yakimenko, S. Meuren, F. Del Gaudio, C. Baumann, A. Fedotov, F. Fiuza, T. Grismayer, M. J. Hogan, A. Pukhov, L. O. Silva, and G. White, "Prospect of studying nonperturbative QED with beam-beam collisions," Phys. Rev. Lett. **122**, 190404 (2019).
[37]A. R. Bell and J. G. Kirk, "Possibility of prolific pair production with high-power lasers," Phys. Rev. Lett. **101**, 200403 (2008).
[38]A. M. Fedotov, N. B. Narozhny, G. Mourou, and G. Korn, "Limitations on the attainable intensity of high power lasers," Phys. Rev. Lett. **105**, 080402 (2010).
[39]S. S. Bulanov, T. Z. Esirkepov, A. G. R. Thomas, J. K. Koga, and S. V. Bulanov, "Schwinger limit attainability with extreme power lasers," Phys. Rev. Lett. **105**, 220407 (2010).
[40]E. N. Nerush, I. Y. Kostyukov, A. M. Fedotov, N. B. Narozhny, N. V. Elkina, and H. Ruhl, "Laser field absorption in self-generated electron-positron pair plasma," Phys. Rev. Lett. **106**, 035001 (2011).
[41]N. V. Elkina, A. M. Fedotov, I. Y. Kostyukov, M. V. Legkov, N. B. Narozhny, E. N. Nerush, and H. Ruhl, "QED cascades induced by circularly polarized laser fields," Phys. Rev. Spec. Top. Accel. Beams **14**, 054401 (2011).
[42]M. Jirka, O. Klimo, S. V. Bulanov, T. Z. Esirkepov, E. Gelfer, S. S. Bulanov, S. Weber, and G. Korn, "Electron dynamics and γ and $e^- e^+$ production by colliding laser pulses," Phys. Rev. E **93**, 023207 (2016).
[43]T. Grismayer, M. Vranic, J. L. Martins, R. A. Fonseca, and L. O. Silva, "Laser absorption via quantum electrodynamics cascades in counter propagating laser pulses," Phys. Plasmas **23**, 056706 (2016).
[44]X.-L. Zhu, T.-P. Yu, Z.-M. Sheng, Y. Yin, I. C. E. Turcu, and A. Pukhov, "Dense GeV electron-positron pairs generated by lasers in near-critical-density plasmas," Nat. Commun. **7**, 13686 (2016).
[45]M. Tamburini, A. D. Piazza, and C. H. Keitel, "Laser-pulse-shape control of seeded QED cascades," Sci. Rep. **7**, 5694 (2017).
[46]A. Gonoskov, A. Bashinov, S. Bastrakov, E. Efimenko, A. Ilderton, A. Kim, M. Marklund, I. Meyerov, A. Muraviev, and A. Sergeev, "Ultrabright GeV photon source via controlled electromagnetic cascades in laser-dipole waves," Phys. Rev. X **7**, 041003 (2017).
[47]T. Grismayer, M. Vranic, J. L. Martins, R. A. Fonseca, and L. O. Silva, "Seeded QED cascades in counterpropagating laser pulses," Phys. Rev. E **95**, 023210 (2017).
[48]A. F. Savin, A. J. Ross, R. Aboushelbaya, M. W. Mayr, B. Spiers, R. H.-W. Wang, and P. A. Norreys, "Energy absorption in the laser-QED regime," Sci. Rep. **9**, 8956 (2019).
[49]I. V. Sokolov, N. M. Naumova, J. A. Nees, and G. A. Mourou, "Pair creation in QED-strong pulsed laser fields interacting with electron beams," Phys. Rev. Lett. **105**, 195005 (2010).
[50]A. G. R. Thomas, C. P. Ridgers, S. S. Bulanov, B. J. Griffin, and S. P. D. Mangles, "Strong radiation-damping effects in a gamma-ray source generated by the interaction of a high-intensity laser with a wakefield-accelerated electron beam," Phys. Rev. X **2**, 041004 (2012).
[51]S. S. Bulanov, C. B. Schroeder, E. Esarey, and W. P. Leemans, "Electromagnetic cascade in high-energy electron, positron, and photon interactions with intense laser pulses," Phys. Rev. A **87**, 062110 (2013).
[52]T. G. Blackburn, C. P. Ridgers, J. G. Kirk, and A. R. Bell, "Quantum radiation reaction in laser–electron-beam collisions," Phys. Rev. Lett. **112**, 015001 (2014).
[53]T. G. Blackburn, A. Ilderton, C. D. Murphy, and M. Marklund, "Scaling laws for positron production in laser–electron-beam collisions," Phys. Rev. A **96**, 022128 (2017).

[54]M. Vranic, J. L. Martins, J. Vieira, R. A. Fonseca, and L. O. Silva, "All-optical radiation reaction at 10^{21}W/cm^2," Phys. Rev. Lett. **113**, 134801 (2014).
[55]M. Vranic, O. Klimo, G. Korn, and S. Weber, "Multi-GeV electron-positron beam generation from laser-electron scattering," Sci. Rep. **8**, 4702 (2018).
[56]S. Meuren, P. H. Bucksbaum, N. J. Fisch, F. Fiúza, S. Glenzer, M. J. Hogan, K. Qu, D. A. Reis, G. White, and V. Yakimenko, "On seminal HEDP research opportunities enabled by colocating multi-petawatt laser with high-density electron beams," arXiv:2002.10051 (2020).
[57]S. Meuren, D. A. Reis, R. Blandford, P. H. Bucksbaum, N. J. Fisch, F. Fiuza, E. Gerstmayr, S. Glenzer, M. J. Hogan, C. Pellegrini, M. E. Peskin, K. Qu, G. White, and V. Yakimenko, "MP3 white paper 2021—Research opportunities enabled by co-locating multi-petawatt lasers with dense ultra-relativistic electron beams," arXiv:2105.11607 (2021).
[58]E. V. Stenson, J. Horn-Stanja, M. R. Stoneking, and T. S. Pedersen, "Debye length and plasma skin depth: Two length scales of interest in the creation and diagnosis of laboratory pair plasmas," J. Plasma Phys. **83**, 595830106 (2017).
[59]C. Bula, K. T. McDonald, E. J. Prebys, C. Bamber, S. Boege, T. Kotseroglou, A. C. Melissinos, D. D. Meyerhofer, W. Ragg, D. L. Burke, R. C. Field, G. Horton-Smith, A. C. Odian, J. E. Spencer, D. Walz *et al.*, "Observation of nonlinear effects in Compton scattering," Phys. Rev. Lett. **76**, 3116 (1996).
[60]D. L. Burke, R. C. Field, G. Horton-Smith, J. E. Spencer, D. Walz, S. C. Berridge, W. M. Bugg, K. Shmakov, A. W. Weidemann, C. Bula, K. T. McDonald, E. J. Prebys, C. Bamber, S. J. Boege, T. Koffas *et al.*, "Positron production in multiphoton light-by-light scattering," Phys. Rev. Lett. **79**, 1626 (1997).
[61]K. Qu, S. Meuren, and N. J. Fisch, "Creating pair plasmas with observable collective effects," Plasma Phys. Controlled Fusion **65**, 034007 (2023).
[62]A. Griffith, K. Qu, and N. J. Fisch, "Particle deceleration for collective QED signatures," Phys. Plasmas **29**, 073104 (2022).
[63]K. Qu, A. Griffith, and N. J. Fisch, "Pair filamentation and laser scattering in beam-driven QED cascades," Phys. Rev. E **109**, 035208 (2024).
[64]A. Griffith, K. Qu, and N. J. Fisch, "Radiation reaction kinetics and collective QED signatures," Phys. Plasmas **31**, 042108 (2024).
[65]E. Cartlidge, "The light fantastic," Science **359**, 382 (2018).
[66]J. Bromage, S.-W. Bahk, I. A. Begishev, C. Dorrer, M. J. Guardalben, B. N. Hoffman, J. Oliver, R. G. Roides, E. M. Schiesser, M. J. Shoup III *et al.*, "Technology development for ultraintense all-OPCPA systems," High Power Laser Sci. **7**, e4 (2019).
[67]C. N. Danson, C. Haefner, J. Bromage, T. Butcher, J.-C. F. Chanteloup, E. A. Chowdhury, A. Galvanauskas, L. A. Gizzi, J. Hein, D. I. Hillier *et al.*, "Petawatt and exawatt class lasers worldwide," High Power Laser Sci. Eng. **7**, e54 (2019).
[68]C. P. Ridgers, C. S. Brady, R. Duclous, J. G. Kirk, K. Bennett, T. D. Arber, A. P. L. Robinson, and A. R. Bell, "Dense electron-positron plasmas and ultraintense γ rays from laser-irradiated solids," Phys. Rev. Lett. **108**, 165006 (2012).
[69]G. Sarri, K. Poder, J. M. Cole, W. Schumaker, A. Di Piazza, B. Reville, T. Dzelzainis, D. Doria, L. A. Gizzi, G. Grittani, S. Kar, C. H. Keitel, K. Krushelnick, S. Kuschel, S. P. D. Mangles, Z. Najmudin, N. Shukla, L. O. Silva, D. Symes, A. G. R. Thomas, M. Vargas, J. Vieira, and M. Zepf, "Generation of neutral and high-density electron-positron pair plasmas in the laboratory," Nat. Commun. **6**, 6747 (2015).
[70]E. Liang, T. Clarke, A. Henderson, W. Fu, W. Lo, D. Taylor, P. Chaguine, S. Zhou, Y. Hua, X. Cen, X. Wang, J. Kao, H. Hasson, G. Dyer, K. Serratto, N. Riley, M. Donovan, and T. Ditmire, "High e+/e- ratio dense pair creation with 10^{21}W.cm^{-2} laser irradiating solid targets," Sci. Rep. **5**, 13968 (2015).
[71]H. Bethe and W. Heitler, "On the stopping of fast particles and on the creation of positive electrons," Proc. R. Soc. London, Ser. A **146**, 83 (1934).
[72]J. W. Motz, H. A. Olsen, and H. W. Koch, "Pair production by photons," Rev. Mod. Phys. **41**, 581 (1969).
[73]C. D. Arrowsmith, P. Simon, P. Bilbao, A. F. A. Bott, S. Burger, H. Chen, F. D. Cruz, T. Davenne, I. Efthymiopoulos, D. H. Froula, A. M. Goillot, J. T. Gudmundsson, D. Haberberger, J. Halliday, T. Hodge, B. T. Huffman, S. Iaquinta, F. Miniati, B. Reville, S. Sarkar, A. A. Schekochihin, L. O. Silva, R. Simpson, V. Stergiou, R. M. G. M. Trines, T. Vieu, N. Charitonidis, R. Bingham, and G. Gregori, "Laboratory realization of relativistic pair-plasma beams," arXiv:2312.05244 (2023).
[74]P. Muggli, "Beam-driven, plasma-based particle accelerators," in *CAS—CERN Accelerator School: Plasma Wake Acceleration* (CERN, Geneva, 2016), pp. 119–142.
[75]N. Shukla, J. Vieira, P. Muggli, G. Sarri, R. Fonseca, and L. O. Silva, "Conditions for the onset of the current filamentation instability in the laboratory," J. Plasma Phys. **84**, 905840302 (2018).
[76]N. Shukla, S. F. Martins, P. Muggli, J. Vieira, and L. O. Silva, "Interaction of ultra relativistic e^-e^+ fireball beam with plasma," New J. Phys. **22**, 013030 (2020).
[77]F. Del Gaudio, T. Grismayer, R. A. Fonseca, W. B. Mori, and L. O. Silva, "Bright γ rays source and nonlinear Breit-Wheeler pairs in the collision of high density particle beams," Phys. Rev. Accel. Beams **22**, 023402 (2019).
[78]W. L. Zhang, T. Grismayer, and L. O. Silva, "Signatures for strong-field QED in the quantum limit of beamstrahlung," Phys. Rev. A **108**, 042816 (2023).
[79]A. Matheron, P. San Miguel Claveria, R. Ariniello, H. Ekerfelt, F. Fiuza, S. Gessner, M. F. Gilljohann, M. J. Hogan, C. H. Keitel, A. Knetsch, M. Litos, Y. Mankovska, S. Montefiori, Z. Nie, B. O'Shea, J. R. Peterson, D. Storey, Y. Wu, X. Xu, V. Zakharova, X. Davoine, L. Gremillet, M. Tamburini, and S. Corde, "Probing strong-field QED in beam-plasma collisions," Commun. Phys. **6**, 141 (2023).
[80]G. Breit and J. A. Wheeler, "Collision of two light quanta," Phys. Rev. **46**, 1087–1091 (1934).
[81]V. I. Ritus, "Quantum effects of the interaction of elementary particles with an intense electromagnetic field," J. Sov. Laser Res. **6**, 497 (1985).
[82]M. Vranic, T. Grismayer, R. A. Fonseca, and L. O. Silva, "Quantum radiation reaction in head-on laser-electron beam interaction," New J. Phys. **18**, 073035 (2016).
[83]N. Neitz and A. Di Piazza, "Stochasticity effects in quantum radiation reaction," Phys. Rev. Lett. **111**, 054802 (2013).
[84]Z. Gong, F. Mackenroth, X. Q. Yan, and A. V. Arefiev, "Radiation reaction as an energy enhancement mechanism for laser-irradiated electrons in a strong plasma magnetic field," Sci. Rep. **9**, 17181 (2019).
[85]S. Meuren, "Light-matter interactions at extreme intensities and densities: Reaching the Schwinger limit," in APS Meeting Abstracts, 2022.
[86]H. Abramowicz, M. Altarelli, R. Aßmann, T. Behnke, Y. Benhammou, O. Borysov, M. Borysova, R. Brinkmann, F. Burkart, K. Büßer, O. Davidi, W. Decking, N. Elkina, H. Harsh, A. Hartin, I. Hartl, B. Heinemann, T. Heinzl, N. TalHod, M. Hoffmann, A. Ilderton, B. King, A. Levy, J. List, A. R. Maier, E. Negodin, G. Perez, I. Pomerantz, A. Ringwald, C. Rödel, M. Saimpert, F. Salgado, G. Sarri, I. Savoray, T. Teter, M. Wing, and M. Zepf, "Letter of intent for the luxe experiment," arXiv:1909.00860 (2019).
[87]K. Poder, M. Tamburini, G. Sarri, A. Di Piazza, S. Kuschel, C. D. Baird, K. Behm, S. Bohlen, J. M. Cole, D. J. Corvan, M. Duff, E. Gerstmayr, C. H. Keitel, K. Krushelnick, S. P. D. Mangles, P. McKenna, C. D. Murphy, Z. Najmudin, C. P. Ridgers, G. M. Samarin, D. R. Symes, A. G. R. Thomas, J. Warwick, and M. Zepf, "Experimental signatures of the quantum nature of radiation reaction in the field of an ultraintense laser," Phys. Rev. X **8**, 031004 (2018).
[88]J. M. Cole, K. T. Behm, E. Gerstmayr, T. G. Blackburn, J. C. Wood, C. D. Baird, M. J. Duff, C. Harvey, A. Ilderton, A. S. Joglekar, K. Krushelnick, S. Kuschel, M. Marklund, P. McKenna, C. D. Murphy, K. Poder, C. P. Ridgers, G. M. Samarin, G. Sarri, D. R. Symes, A. G. R. Thomas, J. Warwick, M. Zepf, Z. Najmudin, and S. P. D. Mangles, "Experimental evidence of radiation reaction in the collision of a high-intensity laser pulse with a laser-field accelerated electron beam," Phys. Rev. X **8**, 011020 (2018).
[89]A. Mercuri-Baron, M. Grech, F. Niel, A. Grassi, M. Lobet, A. D. Piazza, and C. Riconda, "Impact of the laser spatio-temporal shape on Breit-Wheeler pair production," New J. Phys. **23**, 085006 (2021).
[90]E. S. Weibel, "Spontaneously growing transverse waves in a plasma due to an anisotropic velocity distribution," Phys. Rev. Lett. **2**, 83 (1959).
[91]E. G. Harris, "Unstable plasma oscillations in a magnetic field," Phys. Rev. Lett. **2**, 34 (1959).
[92]B. D. Fried, "Mechanism for instability of transverse plasma waves," Phys. Fluids **2**, 337 (1959).
[93]A. Bret, M.-C. Firpo, and C. Deutsch, "Characterization of the initial filamentation of a relativistic electron beam passing through a plasma," Phys. Rev. Lett. **94**, 115002 (2005).

[94]A. Bret, M.-C. Firpo, and C. Deutsch, "Collective electromagnetic modes for beam-plasma interaction in the whole k space," Phys. Rev. E **70**, 046401 (2004).
[95]M. D'Angelo, L. Fedeli, A. Sgattoni, F. Pegoraro, and A. Macchi, "Particle acceleration and radiation friction effects in the filamentation instability of pair plasmas," Mon. N. R. Astron. Soc **451**, 3460 (2015).
[96]M. R. Edwards, N. J. Fisch, and J. M. Mikhailova, "Strongly enhanced stimulated Brillouin backscattering in an electron-positron plasma," Phys. Rev. Lett. **116**, 015004 (2016).
[97]L. Felsen and G. Whitman, "Wave propagation in time-varying media," IEEE Trans. Antennas Propag. **18**, 242–253 (1970).
[98]Y. A. Kravtsov, L. A. Ostrovsky, and N. S. Stepanov, "Geometrical optics of inhomogeneous and nonstationary dispersive media," Proc. IEEE **62**, 1492–1510 (1974).
[99]J. C. AuYeung, "Phase-conjugate reflection from a temporal dielectric boundary," Opt. Lett. **8**, 148–150 (1983).
[100]N. S. Stepanov, "Waves in nonstationary media," Radiophys. Quantum Electron. **36**, 401–409 (1993).
[101]J. T. Mendonça and P. K. Shukla, "Time refraction and time reflection: Two basic concepts," Phys. Scr. **65**, 160 (2002).
[102]F. R. Morgenthaler, "Velocity modulation of electromagnetic waves," IEEE Trans. Microwave Theory Tech. **6**, 167 (1958).
[103]L. A. Ostrovskii and N. S. Stepanov, "Nonresonance parametric phenomena in distributed systems," Radiophys. Quantum Electron. **14**, 387–419 (1971).
[104]C.-L. Jiang, "Wave propagation and dipole radiation in a suddenly created plasma," IEEE Trans. Antennas Propag. **23**, 83–90 (1975).
[105]M. Lampe, E. Ott, and J. H. Walker, "Interaction of electromagnetic waves with a moving ionization front," Phys. Fluids **21**, 42–54 (1978).
[106]E. Yablonovitch, "Spectral broadening in the light transmitted through a rapidly growing plasma," Phys. Rev. Lett. **31**, 877 (1973).
[107]C. J. Joshi, C. Clayton, K. Marsh, D. Hopkins, A. Sessler, and D. Whittum, "Demonstration of the frequency upshifting of microwave radiation by rapid plasma creation," IEEE Trans. Plasma Sci. **18**, 814–818 (1990).
[108]S. P. Kuo, "Frequency up-conversion of microwave pulse in a rapidly growing plasma," Phys. Rev. Lett. **65**, 1000 (1990).
[109]R. Savage, R. Brogle, W. Mori, and C. Joshi, "Frequency upshifting and pulse compression via underdense relativistic ionization fronts," IEEE Trans. Plasma Sci. **21**, 5–19 (1993).
[110]N. Yugami, T. Niiyama, T. Higashiguchi, H. Gao, S. Sasaki, H. Ito, and Y. Nishida, "Experimental observation of short-pulse upshifted frequency microwaves from a laser-created overdense plasma," Phys. Rev. E **65**, 036505 (2002).
[111]A. Nishida, N. Yugami, T. Higashiguchi, T. Otsuka, F. Suzuki, M. Nakata, Y. Sentoku, and R. Kodama, "Experimental observation of frequency upconversion by flash ionization," Appl. Phys. Lett. **101**, 161118 (2012).
[112]I. Geltner, Y. Avitzour, and S. Suckewer, "Picosecond pulse frequency upshifting by rapid free-carrier creation in znse," Appl. Phys. Lett. **81**, 226 (2002).
[113]Y. Avitzour, I. Geltner, and S. Suckewer, "Laser pulse frequency shifting by ionization and recombination fronts in semiconductor plasma," J. Phys. B **38**, 779 (2005).
[114]W. L. Kruer, "Ponderomotive and thermal filamentation of laser light," Comments Plasma Phys. Controlled Fusion **9**, 63 (1985).
[115]P. Kaw, G. Schmidt, and T. Wilcox, "Filamentation and trapping of electromagnetic radiation in plasmas," Phys. Fluids **16**, 1522 (1973).
[116]P. E. Young, H. A. Baldis, R. P. Drake, E. M. Campbell, and K. G. Estabrook, "Direct evidence of ponderomotive filamentation in a laser-produced plasma," Phys. Rev. Lett. **61**, 2336 (1988).
[117]E. Sobacchi, Y. Lyubarsky, A. M. Beloborodov, L. Sironi, and M. Iwamoto, "Saturation of the filamentation instability and dispersion measure of fast radio bursts," Astrophys. J. Lett. **943**, L21 (2023).
[118]Z. Gong, K. Z. Hatsagortsyan, and C. H. Keitel, "Electron polarization in ultrarelativistic plasma current filamentation instabilities," Phys. Rev. Lett. **130**, 015101 (2023).
[119]D. Seipt, D. Del Sorbo, C. P. Ridgers, and A. G. R. Thomas, "Theory of radiative electron polarization in strong laser fields," Phys. Rev. A **98**, 023417 (2018).
[120]Y.-F. Li, R. Shaisultanov, K. Z. Hatsagortsyan, F. Wan, C. H. Keitel, and J.-X. Li, "Ultrarelativistic electron-beam polarization in single-shot interaction with an ultraintense laser pulse," Phys. Rev. Lett. **122**, 154801 (2019).
[121]Y.-F. Li, Y.-Y. Chen, K. Z. Hatsagortsyan, and C. H. Keitel, "Helicity transfer in strong laser fields via the electron anomalous magnetic moment," Phys. Rev. Lett. **128**, 174801 (2022).
[122]V. Yakimenko, L. Alsberg, E. Bong, G. Bouchard, C. Clarke, C. Emma, S. Green, C. Hast, M. J. Hogan, J. Seabury, N. Lipkowitz, B. O'Shea, D. Storey, G. White, and G. Yocky, "FACET-II facility for advanced accelerator experimental tests," Phys. Rev. Accel. Beams **22**, 101301 (2019).
[123]T. D. Arber, K. Bennett, C. S. Brady, A. Lawrence-Douglas, M. G. Ramsay, N. J. Sircombe, P. Gillies, R. G. Evans, H. Schmitz, A. R. Bell *et al.*, "Contemporary particle-in-cell approach to laser-plasma modelling," Plasma Phys. Controlled Fusion **57**, 113001 (2015).
[124]A. Gonoskov, S. Bastrakov, E. Efimenko, A. Ilderton, M. Marklund, I. Meyerov, A. Muraviev, A. Sergeev, I. Surmin, and E. Wallin, "Extended particle-in-cell schemes for physics in ultrastrong laser fields: Review and developments," Phys. Rev. E **92**, 023305 (2015).
[125]A. Di Piazza, M. Tamburini, S. Meuren, and C. H. Keitel, "Implementing nonlinear Compton scattering beyond the local-constant-field approximation," Phys. Rev. A **98**, 012134 (2018).
[126]G. Torgrimsson, "Loops and polarization in strong-field QED," New J. Phys. **23**, 065001 (2021).
[127]T. G. Blackburn, B. King, and S. Tang, "Simulations of laser-driven strong-field QED with Ptarmigan: Resolving wavelength-scale interference and γ-ray polarization," Phys. Plasmas **30**, 093903 (2023).
[128]A. J. Gonsalves, K. Nakamura, J. Daniels, C. Benedetti, C. Pieronek, T. C. H. de Raadt, S. Steinke, J. H. Bin, S. S. Bulanov, J. van Tilborg, C. G. R. Geddes, C. B. Schroeder, C. Tóth, E. Esarey, K. Swanson, L. Fan-Chiang, G. Bagdasarov, N. Bobrova, V. Gasilov, G. Korn, P. Sasorov, and W. P. Leemans, "Petawatt laser guiding and electron beam acceleration to 8 GeV in a laser-heated capillary discharge waveguide," Phys. Rev. Lett. **122**, 084801 (2019).
[129]B. Miao, J. E. Shrock, L. Feder, R. C. Hollinger, J. Morrison, R. Nedbailo, A. Picksley, H. Song, S. Wang, J. J. Rocca, and H. M. Milchberg, "Multi-GeV electron bunches from an all-optical laser wakefield accelerator," Phys. Rev. X **12**, 031038 (2022).
[130]K. V. Grafenstein, F. M. Foerster, F. Haberstroh, D. Campbell, F. Irshad, F. C. Salgado, G. Schilling, E. Travac, N. Weiße, M. Zepf, A. Döpp, and S. Karsch, "Laser-accelerated electron beams at 1 GeV using optically-induced shock injection," Sci. Rep. **13**, 11680 (2023).
[131]T. V. Liseykina, S. V. Popruzhenko, and A. Macchi, "Inverse Faraday effect driven by radiation friction," New J. Phys. **18**, 072001 (2016).
[132]P. J. Bilbao and L. O. Silva, "Radiation reaction cooling as a source of anisotropic momentum distributions with inverted populations," Phys. Rev. Lett. **130**, 165101 (2023).
[133]V. Zhdankin, M. W. Kunz, and D. A. Uzdensky, "Synchrotron firehose instability," Astrophys. J. **944**, 24 (2023).